
ELECTRIC AND MAGNETIC
PROPERTIES OF MATERIALS

Features of the Electrical and Photoelectrical Properties of Nanocrystalline Indium and Zinc Oxide Films

T. V. Belysheva^a, M. I. Ikim^b, A. S. Il'in^{c, d, *}, P. K. Kashkarov^{c, d, e}, M. N. Martyshov^c,
Y. Paltiel^f, L. I. Trakhtenberg^b, N. P. Fantina^c, and P. A. Forsh^{c, d}

^aKarpov Institute of Physical Chemistry, Moscow, 103064 Russia

^bSemenov Institute of Chemical Physics, Russian Academy of Sciences, Moscow, 117977 Russia

^cMoscow State University, Moscow, 119991 Russia

^dNational Research Center “Kurchatov Institute”, Moscow, 123098 Russia

^eMoscow University of Physics and Technology, Dolgoprudnyi, Moscow oblast, 141701 Russia

^fApplied Physics Department, Center for Nano-Science and Nano-Technology,
The Hebrew University of Jerusalem, Jerusalem, 91904 Israel

*e-mail: as.ilin@physics.msu.ru

Received March 18, 2016

Abstract—Electrical and photoelectrical properties of nanocrystalline zinc oxide and indium oxide films are studied. For these oxides the temperature dependences of conductance are observed to be consisting of two parts with different activation energy. Also photoconductivity relaxation of the oxides can be described by a sum of two exponential functions. The spectral dependencies of nanocrystalline zinc oxide and indium oxide photoconductivity are presented. The photoconductivity arises as samples are illuminated with energy less than band gap. The data are discussed on the basis of model by which the localized states in the band gap play major role.

Keywords: metal oxides, temperature dependence of the conductivity, photoconductivity, localized levels

DOI: 10.1134/S1990793116050171

INTRODUCTION

At present, metal oxides are considered to be promising materials having a wide application in various technical fields. Some of the most used are nanocrystalline zinc oxide (ZnO) and indium oxide (In₂O₃). For instance, indium oxide is applied in the fabrication of displays in mobile devices, solar cells, and gas sensors [1–4]. Zinc oxide is widely used in optoelectronics, photo sensor devices, microelectronics [5–8]. The usage of mixtures of these oxides for manufacturing gas sensors is considered to be promising [9].

The properties of oxides strongly depend on the structure and synthesis methods. Nanocrystalline indium and zinc oxides have an appreciable specific surface area, contain a large number of defect states, and are uncontrollably doped semiconductors of the n-type conductivity (see [2] and references therein and also [10, 11]). The character of the temperature dependences of the conductivity of these materials is largely determined by conditions under which the samples were synthesized and also the temperature range in which the measurements were performed. In particular, depending on the synthesis method, structure, and temperature range, the temperature depen-

dences of the conductivity of indium and zinc oxides can be activated with one activation energy [12, 13] or have two regions with different activation energies [14–16], or the conductivity can even decrease with increasing temperature in some temperature range [14, 17, 18]. An unambiguous interpretation of the observed temperature dependences of the ZnO and In₂O₃ conductivities is absent in the literature. Thus, in some publications it is assumed that a change in the activation energy is related to the adsorption and desorption of gas molecules, in particular, oxygen from the sample surfaces [18, 19]. In other publications it is considered that this temperature dependence is characteristic of unordered semiconductors and is explained by the randomly changing potential along the semiconductor [14, 20].

Researchers also make many efforts to investigate the photoconductivity of nanostructured semiconductors of metal oxides. In order to explain the phenomena of long-term relaxation of the photoconductivity and the residual photoconductivity, which are characteristic of these semiconductors, various models are being developed [12, 18, 21–23]. As for nanocrystalline metal oxides, these phenomena have been mostly studied in zinc oxide. However, the unambigu-

ous explanation of the observed dependences of relaxation of the photoconductivity in nanocrystalline metal oxides has been absent so far. This is very likely to be due to the absence of a combined study of the conductivity and relaxation of the photoconductivity in samples of various nanocrystalline metal oxides.

In this work, the temperature dependences of the dark conductivity, the spectral dependences of the photoconductivity, and the photoconductivity decay of nanocrystalline indium and zinc oxides with approximately the same structural parameters were studied in detail to establish some general regularities inherent in nanocrystalline metal oxides.

EXPERIMENTAL

Oxide films were synthesized from In_2O_3 and ZnO powders. The average size of oxide nanocrystals in the source powder, which was determined by electron microscopy and powder X-ray diffraction, was 50–80 nm [9]. In order to form the films, the oxide powders were mixed with some amount of water, after which they were ground in a mortar until a homogeneous paste was obtained. Then the paste was deposited on a thick glass slide and annealed for 3 h in the air atmosphere, the temperature being gradually increased from 120 to 550°C.

For the measurement of the electrical and photoelectrical characteristics 3 mm long gold contacts were deposited on the upper surface of the films. The distance between the contact areas was 0.5 mm. All measurements were carried out in the air.

The temperature dependences of the dark conductivity of the samples were measured in the temperature range of 270–470 K. For the measurement of the photoelectrical characteristics of the samples under study an ultraviolet light diode with a wavelength of 385 nm and an intensity of 5 mW/cm² was used as a radiation source. The photoconductivity value (σ_{ph}) was found as a difference of sample conductivities on light irradiation (σ_{ill}) and the dark conductivity (σ_{d})

$$\sigma_{\text{ph}} = \sigma_{\text{ill}} - \sigma_{\text{d}}$$

The spectral dependences of the photoconductivity were measured by light irradiation with monochromatic light in the range 380–610 nm using a powerful DKSL-1000 xenon lamp and an MDR-12 monochromator. The intensity of monochromatic light incident on the sample was approximately 2 mW/cm² in the whole spectral range.

RESULTS AND DISCUSSION

The temperature dependences of the conductivity of the studied In_2O_3 and ZnO samples are shown in Fig. 1. As seen from the figure, in the whole temperature range studied the dark conductivity of In_2O_3 is much higher than the conductivity of ZnO . It should be noted that in the temperature dependences of the

conductivity of each sample two activation regions can be distinguished in each of them. They are described by the expression

$$\sigma(T) = \sigma_0 \exp\left(-\frac{E_a}{kT}\right),$$

where k is the Boltzmann constant and σ_0 is the coefficient independent (or weakly dependent) on the temperature.

The first activation region is observed at high temperatures ($T > 380$ – 390 K). The activation energy in this region is $E_a^{(1)} = 0.09$ eV for In_2O_3 and $E_a^{(1)} = 0.48$ eV for zinc oxide. At temperatures below 370 K the second activation region is observed. Here the activation energy $E_a^{(2)} = 0.03$ eV for In_2O_3 and $E_a^{(2)} = 0.36$ eV for ZnO . It is worth noting that for both oxides the activation energy of the second region is lower than that of the first one. Similar data for In_2O_3 were obtained in [24].

The semiconductor conductivity can be presented in the form [25]

$$\sigma = e\mu n, \quad (1)$$

where e is the electron charge, μ and n are the electron mobility and concentration respectively. Note that formula (1) is written in the assumption that the conductivity is determined by electrons, which is valid for nanocrystalline In_2O_3 and ZnO . For a non-degenerate semiconductor the electron concentration is expressed as [25]

$$n = N_c \exp\left(-\frac{E_c - F}{kT}\right).$$

Here N_c is the effective density of states in the conduction band, E_c and F are the energies of the bottom of the conduction band and the Fermi level respectively. If the electron mobility is assumed to be independent of the temperature (or only a weak dependence determined by the scattering mechanism is observed), then the activation energy of the conductivity, which is present in formula (1), is determined by the Fermi level relative to the bottom of the conduction band, i.e. $E_a = E_c - F$.

A temperature dependent change in the activation energy can be explained by a shift of the Fermi level. Two characteristic activation regions in the temperature dependences of the conductivity (see, e.g., [26]) are often described in the assumption of the presence of one simple (i.e., occurring only in two charge states: neutral and positively charged) donor level in the semiconductor. In the low temperature range the donor level is ionized (this mode is described by the activation dependence of the conductivity with the activation energy equal to a half of the energy distance between the donor level and the bottom of the conduction band), and with an increase in the temperature the electron concentration, and hence, the conductivity increase due to the electron excitation from

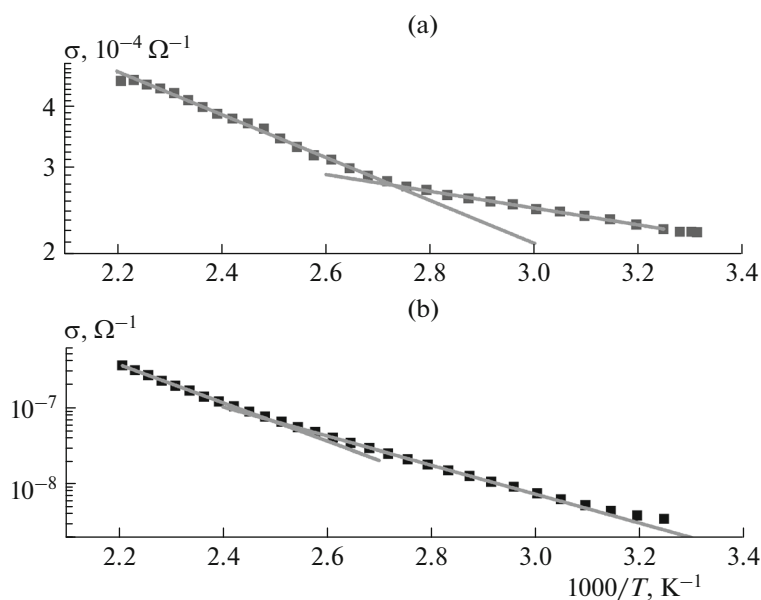


Fig. 1. Temperature dependences of the conductivity of nanocrystalline indium oxide (a) and zinc oxide (b) films. Lines show the approximations of the temperature dependences by the activation law.

the valence band to the conduction band. Here the second activation region with a much higher activation energy is observed.

In our case, however, this explanation is unlikely because in the studied temperature range, the probability of the transition to the second mode (the transition of electrons from the valence band to the conduction band) is extremely low because for this mode much higher temperatures are usually required. Moreover, in this model a region must be where the conductivity practically does not depend on the temperature. This region must be observed on passing from the first mode to the second when all donors become ionized and an increase in the electron concentration, and consequently, the conductivity due to the inflow of electrons from the valence band practically does not occur. A plateau in the temperature dependence of the conductivity in Fig. 1 is not observed either. In [24] the assumption was made that there was an energy dispersion of traps; furthermore, an alteration of the transfer mechanism is possible. At low temperatures the tunnel mechanism mainly works and at elevated temperatures the mechanism is activation transitions.

For the interpretation of our experimental data it is reasonable to assume that there are two simple donor levels. The origin of these levels can be different. It can be both defect states inside nanocrystals and surface states at the nanocrystal boundaries. It can also be the states of oxygen vacancies. Although oxygen vacancies in metal oxides are not simple centers and not described by the Fermi–Dirac distribution used below for simple centers, the situation must also be qualitatively close to that described below.

For the simulation we assume that there are two simple donor levels with the energies E_1 , E_2 and concentrations N_1 , N_2 respectively. For the clearness we consider the E_1 level to be closer to the bottom of the conduction band than the E_2 level. A change in the position of the Fermi level with increasing temperature can be determined from the equation of electroneutrality

$$N_c \exp\left(\frac{F - E_c}{kT}\right) = \frac{N_1}{1 + (g_{11}/g_{10}) \exp[(F - E_1)/kT]} + \frac{N_2}{1 + (g_{21}/g_{20}) \exp[(F - E_2)/kT]}, \quad (2)$$

where g_{i0} and g_{i1} are the degeneration factors of the unoccupied and occupied i -th level ($i = 1, 2$). Owing to that in equation (2) we deal with n -type semiconductors and neglect the positive charge of holes and the negative charge of acceptor levels whose existence cannot be excluded. Let us introduce the following designations:

$$x = \exp\frac{F - E_c}{kT}, \quad a = \frac{g_{11}}{g_{10}} \exp\frac{E_c - E_1}{kT}, \\ b = \frac{g_{21}}{g_{20}} \exp\frac{E_c - E_1}{kT}, \quad n_1 = \frac{N_1}{N_c}, \quad n_2 = \frac{N_2}{N_c}.$$

Then equation of electroneutrality (2) can be rewritten as follows:

$$x = \frac{n_1}{1 + ax} + \frac{n_2}{1 + bx}. \quad (3)$$

At the lowest temperatures the donor levels are not yet ionized and the Fermi level lies higher than both donor levels [25]. Since the upper level is first ionized, in the assumption of low temperatures in equation (3)

the occurrence of the second level ($\exp \frac{F - E_2}{kT} \gg 1$,

$N_2^+ = 0$) can be neglected, i.e. it is possible to consider that the second level is completely filled with electrons and is electroneutral. Then equation (3) can be written in the form

$$x = \frac{n_1}{1 + ax}. \quad (4)$$

Under the condition $(4an_1)^{1/2} \gg 1$, which is satisfied at sufficiently low temperatures, it is easy to obtain

$$n = N_c x \sim a^{-1/2} = \exp\left(-\frac{E_c - E_1}{2kT}\right). \quad (5)$$

According to formulas (1) and (5), the conductivity has the activation character with the activation energy

$$E_a^{(1)} = \frac{E_c - E_1}{2}. \quad (6)$$

When the Fermi level becomes lower than the E_1 level (this occurs with an increase in the temperature), the E_2 level starts to take part in the electron generation. Let us consider the case when the Fermi level is lower in energy than the E_1 level so that $\exp \frac{F - E_1}{kT} \ll 1$. Then the first summand of equation (3) can be expanded in series, being limited to the first two terms

$$x = n_1(1 - ax) + \frac{n_2}{(1 + bx)}.$$

When $4(n_1 + n_2)b \gg (n_1b - 1)^2$, and $an_1 \ll 1$ (the second level starts to be ionized at relatively high temperatures), we obtain

$$n = N_c x \sim b^{-1/2} = \exp\left(-\frac{E_c - E_2}{2kT}\right).$$

This means that in this region the conductivity has the activation character with an activation energy

$$E_a^{(2)} = \frac{E_c - E_2}{2}. \quad (7)$$

Thus, the E_1 , E_2 energies of the levels and their concentrations N_1 , N_2 can be such that with an increase in the temperature in the temperature dependence of the conductivity the activation energy changes. At low temperatures it is determined by formula (6), and at high temperatures by formula (7). Just this behavior is observed for the studied nanocrystalline indium and zinc oxides.

It should be noted that depending on the position of donor levels, their concentrations in the considered temperature range, other characteristic regions can be observed in the temperature dependence of the conductivity. Thus, for instance, if the E_1 and E_2 levels are located sufficiently far from each other, then there is a temperature range in which the E_1 level is completely ionized and the electron throw from the E_2 level to the conduction band is not started yet. In solution (4) this mode corresponds to the condition $4an_1 \ll 1$, here $x = n_1$. This means that the electron concentration does not change with increasing temperature. If we assume that due to the scattering the mobility decreases with increasing temperature, then according to formula (1), in this temperature range the conductivity also decreases with increasing temperature. As already noted, in some publications this temperature dependence of the conductivity in metal oxides is mentioned [14, 18].

Now we turn to the consideration of the photoelectrical properties. Figure 2 depicts the spectral dependences of the photoconductivity of the studied samples. According to the literature data [27], the band gap of zinc oxide is near 3.4 eV, and for indium oxide the band gap is not clearly determined so far, however, it is known that it exceeds 2.8 eV [28–30]. However, for both In_2O_3 and ZnO , as follows from Fig. 2, the photoconductivity appears at quantum energies smaller than the band gap. This can give evidence of the presence of localized states in the band gap, which contribute to the photoconductivity of the studied oxides.

It is worth noting that not only donor levels determining the temperature dependence of the conductivity can be these localized states. The point is that there can be localized states that do not contribute to equation of electroneutrality (2) in the considered temperature range (in which the dark conductivity was studied), and hence, do not affect the temperature course of the Fermi level. For instance, this can be the donor level lying much farther from the bottom of the conduction band than the E_2 level and is neutral or the level (including the acceptor one) whose concentration of states is negligible in comparison with the concentrations of states of levels contributing to the conductivity. However, these levels can contribute to the photoconductivity, and consequently, determine the spectral dependence of the photoconductivity at quantum energies smaller than the band gap.

The taking into account of the localized states makes it possible to elucidate the question about the mechanisms determining relaxation of the photoconductivity of the studied samples. Figure 3 shows the photoconductivity decay curves for the indium oxide and zinc oxide samples after their irradiation with ultraviolet light. Before the experiment the samples were light irradiated for 1 h until the attainment of the stationary state of the photoconductivity. Dashed lines

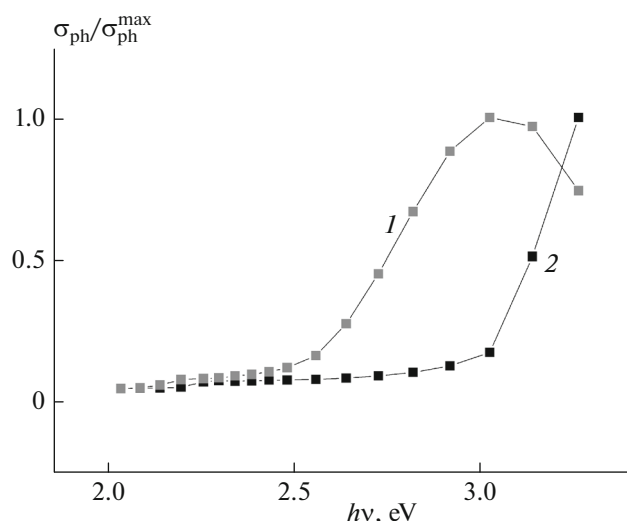


Fig. 2. Normalized spectral dependences of the photoconductivity of nanocrystalline indium oxide (1) and zinc oxide (2) films.

in Fig. 3 correspond to the dark conductivity of the samples.

Relaxation of the photoconductivity of both samples can be approximated by the following formula:

$$\sigma(t) = A_1 \exp\left(-\frac{t}{\tau_1}\right) + A_2 \exp\left(-\frac{t}{\tau_2}\right), \quad (8)$$

where A_1 and A_2 are the pre-exponential factors, τ_1 and τ_2 are the effective relaxation times of the photoconductivity. The τ_1 and τ_2 relaxation times (17400 and 900 s for In_2O_3 and 1900 and 150 s for ZnO respectively) characterizing the slow and fast processes, are

larger for indium oxide than for a zinc oxide by an almost order of magnitude.

The observed slow relaxation of the photoconductivity can be explained if we assume that the charge carrier recombination proceeds through two localized levels in the band gap. If the electron exchange between the levels is neglected, then one exponent in formula (8) describes the recombination through a more shallow level and another through a deeper level. It is difficult to say what levels work as the recombination centers in studied In_2O_3 and ZnO. However, it is possible to suppose that these levels are sufficiently shallow because the shallow levels work more as traps rather than the recombination centers.

If the photoconductivity decay times τ_1 and τ_2 are considered to be independent of the concentration of non-equilibrium charge carriers, then these times coincide with the stationary lifetimes in the recombination through the corresponding level. In this case, the τ_1 and τ_2 values are determined by the Shockley–Read–Hall formula [31]. According to this formula, the recombination proceeds faster through the level lying closer to the middle of the band gap. It is possible to assume that in ZnO the levels through which the recombination proceeds lie closer to the middle of the band gap than those in In_2O_3 , therefore in ZnO the photoconductivity decay is faster.

CONCLUSIONS

In the work the electrical and photoelectrical properties of nanocrystalline zinc and indium oxides with nanocrystal sizes of 50–80 nm were studied. It is found that the temperature dependences of nanocrystalline In_2O_3 and ZnO in the temperature range from 270 to 470 K consist of two activation regions with dif-

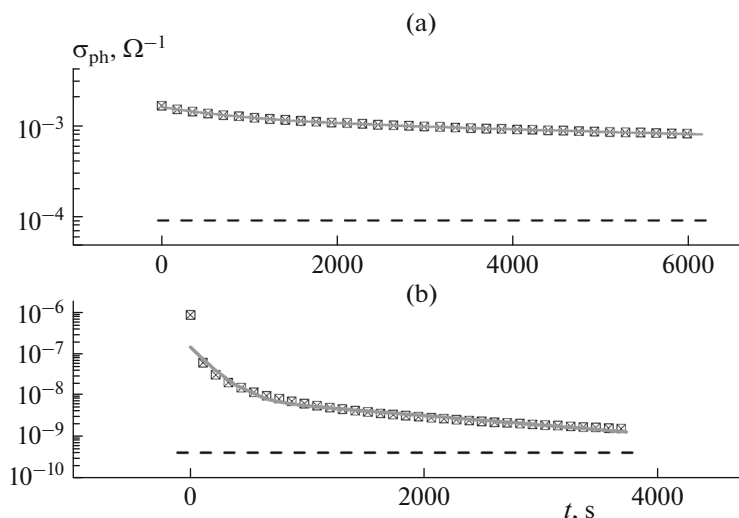


Fig. 3. Relaxation of the photoconductivity of nanocrystalline In_2O_3 (a) and ZnO (b) films. The line shows the approximations of decays by a sum of exponents. The dashed line shows the dark conductivity of the samples.

ferent activation energies. The obtained temperature dependences of the conductivity can be explained by the presence of two effective donor levels. In the temperature range below 370 K the activation energy is lower than that at higher temperatures. The lower activation energy describes the ionization of the shallow donor level whereas the higher activation energy is related to a deeper level ionization. It is shown that temperature dependence may include non-activation regions in dependence on the energy positions of electronic levels and their concentration. The consideration has a general character therefore the proposed model can also be used to explain other temperature dependences of the conductivity of nanocrystalline metal oxides, which are available in the literature.

From the analysis of the spectral dependences of the photoconductivity of nanocrystalline In_2O_3 and ZnO it is possible to conclude that apart from two localized levels determining the temperature dependence of the conductivity, other localized states are also present in the band gap. The latter provide the photoconductivity of nanocrystalline In_2O_3 and ZnO in the quantum energy range smaller than the band gap.

Relaxation of the photoconductivity in the studied samples can be described by a sum of two exponents. The approximation makes it possible to distinguish the slow and fast parts of the decay. It is possible to assume that the charge carrier recombination proceeds through two localized levels in the band gap. The slow part of the decay can be determined by the recombination through a shallow localized level and the fast part of the decay is associated with the recombination through a deep localized level.

ACKNOWLEDGMENTS

The work was supported by the Russian Scientific Foundation (grant no. 14-19-00781) and the Russian Foundation for Basic Research (project no. 16-32-60060 mol_a_dk).

REFERENCES

1. A. S. Il'in, N. P. Fantina, M. N. Martyshov, P. A. Forsh, A. S. Vorontsov, M. N. Rumyantseva, A. M. Gas'kov, and P. K. Kashkarov, *Tech. Phys. Lett.* **41**, 252 (2015). doi 10.1134/S1063785015030074
2. O. Bierwagen, *Semicond. Sci. Technol.* **30**, 1088 (2015). doi 10.1088/0268-1242/30/2/024001
3. G. Shen, B. Liang, X. Wang, et al., *Am. Chem. Soc. Nano* **5**, 6148 (2011). doi 10.1021/nn2014722
4. E. A. Forsh, A. V. Marikutsa, M. N. Martyshov, P. A. Forsh, M. N. Rumyantseva, A. M. Gas'kov, and P. K. Kashkarov, *Nanotechnol. Russ.* **7**, 164 (2012). doi 10.1134/S1995078012020073
5. O. Lupan, V. V. Ursaki, G. Chai, et al., *Sens. Actuators. B: Chem.* **144**, 56 (2010). doi 10.1016/j.snb.2009.10.038
6. L. Li, T. Zhai, Y. Bando, and D. Golberg, *Nano Energy* **1**, 91 (2012). doi 10.1016/j.nanoen.2011.10.005
7. H. Ham, G. Shen, J. H. Cho, et al., *Chem. Phys. Lett.* **404**, 69 (2005). doi 10.1016/j.nanoen.2011.10.005
8. J. I. Sohn, S. S. Choi, S. M. Morris, et al., *Nano Lett.* **10**, 4316 (2010). doi 10.1021/nl1013713
9. L. I. Trakhtenberg, G. N. Gerasimov, V. F. Gromov, et al., *Sens. Actuators B: Chem.* **187**, 514 (2013). doi 10.1016/j.snb.2013.03.017
10. M. D. McCluskey and S. J. Jokela, *J. Appl. Phys.* **106**, 1 (2009). doi 10.1063/1.3216464
11. S. Zhang, S.-H. Wei, and A. Zunger, *Phys. Rev.* **63**, 1 (2001). doi 10.1103/PhysRevB.63.075205
12. S. A. Studenikin, N. Golego, and M. Cocivera, *J. Appl. Phys.* **87**, 2413 (2000). doi 10.1063/1.372194
13. *Semiconductors*, Ed. by N. B. Hannay (Reinhold, New York, 1959; Inostr. Liter., Moscow, 1962).
14. N. A. Vorob'eva, M. N. Rumyantseva, P. A. Forsh, and A. M. Gas'kov, *Semiconductors* **47**, 650 (2013).
15. E. A. Forsh, A. V. Marikutsa, M. N. Martyshov, et al., *Thin Solid Films* **558**, 320 (2014). doi 10.1016/j.tsf.2014.02.064
16. E. A. Forsh, A. V. Marikutsa, M. N. Martyshov, P. A. Forsh, M. N. Rumyantseva, A. M. Gas'kov, and P. K. Kashkarov, *J. Exp. Theor. Phys.* **111**, 653 (2010). doi 10.1134/S106377611010016X
17. T. V. Belysheva, G. N. Gerasimov, V. F. Gromov, E. Yu. Spiridonova, and L. I. Trakhtenberg, *Russ. J. Phys. Chem. A* **84**, 1554 (2010). doi 10.1134/S0036024410090207
18. S. E. BurrueI-Ibarra, C. Cruz-Vazquez, R. Bernal, et al., *J. Electron. Mater.* **45**, 1007 (2016). doi 10.1007/s11664-015-4199-1
19. P. P. Sahay and R. K. Nath, *Sens. Actuators B: Chem.* **134**, 654 (2008). doi 10.1016/j.snb.2008.06.006
20. M. K. Sheinkman and A. Ya. Shik, *Sov. Phys. Semicond.* **10**, 128 (1976).
21. J. Reemts and A. Kittel, *J. Appl. Phys.* **101**, 013709 (2007). doi 10.1063/1.2407264
22. Q. H. Li, T. Gao, Y. G. Wang, and T. H. Wang, *Appl. Phys. Lett.* **86**, 123117 (2005). doi 10.1063/1.1883711
23. E. A. Forsh, A. S. Il'in, M. N. Martyshov, P. A. Forsh, and P. K. Kashkarov, *Nanotechnol. Russ.* **9**, 618 (2014). doi 10.1134/S1995078014060093
24. T. V. Belysheva, A. K. Gatin, M. V. Grishin, M. I. Ikim, V. M. Matyuk, S. Y. Sarvadai, L. I. Trakhtenberg, and B. R. Shub, *Russ. J. Phys. Chem. B* **9**, 733 (2015). doi 10.1134/S1990793115050048
25. V. L. Bonch-Bruevich and S. G. Kalashnikov, *Semiconductor Physics* (Fizmatlit, Moscow, 1977) [in Russian].
26. G. I. Epifanov, *Solid State Physics* (Vyssh. Shkola, Moscow, 1977) [in Russian].
27. B. K. Meyer, H. Alves, D. M. Hofmann, et al., *Phys. Status Solidi B* **241**, 227 (2004). doi 10.1002/pssb.200490002
28. A. Walsh, J. L. F. da Silva, S. H. Wei, et al., *Phys. Rev. Lett.* **100**, 2 (2008). doi 10.1103/PhysRevLett.100.167402
29. P. D. C. King, T. D. Veal, F. Fuchs, et al., *Phys. Rev. B* **79**, 205211 (2009). doi 10.1103/PhysRevB.79.205211
30. E. A. Forsh, A. M. Abakumov, V. B. Zaytsev, et al., *Thin Solid Films* **595**, 25 (2015). doi 10.1016/j.tsf.2015.10.053
31. S. M. Ryvkin, *Photoelectric Phenomena in Semiconductors* (Fizmatgiz, Moscow, 1963) [in Russian].

Translated by L. Chernikova